

# Rank-One Tensor Modeling Approach to Joint Channel and Symbol Estimation in Two-Hop MIMO Relaying Systems

Bruno Sokal, André L. F. de Almeida and Martin Haardt

**Abstract**—This paper proposes two semi-blind receivers for joint channel and symbol estimation in MIMO relay-based communication systems. These receivers are developed for a two-hop system, assuming a tensor coding at the source and relay nodes. The central idea of the proposed approach is on the rank-one tensor modeling of the received signal, which allows the use of efficient estimation algorithms. The first receiver utilizes an iterative solution based on the alternating least squares (ALS) algorithm, while the second provides closed-form estimations of the channel and symbol matrices from a truncated higher order singular value decomposition (T-HOSVD). The proposed approach has a lower complexity compared to the receiver developed in a previous work, while providing remarkable performance.

**Keywords**—MIMO systems, Cooperative communications, tensor decompositions, semi-blind receiver.

## I. INTRODUCTION

The use of relay stations in multiple input multiple output (MIMO) wireless communication systems has shown to be a promising technique to combat signal propagation effects, such as path loss and shadowing, leading to increased capacity and coverage in wireless communication systems [1], [2], [3]. In this context, amplify-and-forward (AF) relaying is an attractive solution, being preferable when complexity and/or latency issues are of importance [3]. The benefits of relay-assisted wireless communications strongly rely on the accuracy of the channel state information (CSI) for all the links involved in the communication process. Moreover, the use of precoding techniques at the source and/or destination [4], [5] often requires the instantaneous CSI knowledge of all links.

Since the pioneering work [6], the use of tensor decompositions has been widely studied for modeling wireless communication systems. The practical motivation for tensor modeling comes from the fact that one can simultaneously benefit from multiple signal diversities, like space, time and frequency diversities, for instance. Moreover, tensor approaches offer the possibility of using blind/semi-blind techniques for channel and symbol estimation under uniqueness conditions more relaxed than those with conventional matrix-based solutions.

In the context of wireless communications, tensor decompositions have proved useful in the development of

semi-blind receivers to solve problems of channel and symbol estimation [7], [8], [9]. In the specific case of MIMO relaying communication systems, a few works have proposed tensor modeling based receivers (see, e.g. [10], [11], [12], [13]). In [13], the authors provide a generalization of [12] by assuming a full tensor coding at the source and relay nodes. Therein, two semi-blind receivers are proposed by exploiting a Nested Tucker model for the received signal tensor. The first one relies on an iterative alternating least squares (ALS) algorithm while the second one consists of a two-stage Kronecker factorization algorithm based on two successive singular value decompositions (SVDs). The main limitation of the approach of [13] is the high computational complexity of the ALS-based receiver, which is intrinsic to the Nested Tucker model, requiring extensive matrix products and pseudo-inverse computations at every iteration. On the other hand, the Kronecker factorization receiver is suboptimal since it divides channel and symbol estimations in two steps, the latter being dependent on the accuracy of the first.

In this paper, we present two semi-blind receivers for joint channel and symbol estimation in two-hop MIMO communication systems. Following the system model and assumptions of [13], we start from a Nested Tucker tensor model and recast the received signal after space-time combining as a rank-one third-order tensor (i.e. a standard PARAFAC model), whose factors are the source-relay channel, relay-destination channel, and symbol vectors. An orthogonal design for the combined source-relay coding structure is proposed, which translates space-time combining into matched filtering. Exploiting the conceptual simplicity of the resulting PARAFAC model, two efficient semi-blind receivers are derived to jointly estimate the channels and symbols. The first receiver utilizes an iterative solution based on the alternating least squares (ALS) algorithm, while the second provides closed-form estimations of the channel and symbol matrices from a truncated higher order singular value decomposition (T-HOSVD). The proposed receivers have a lower complexity compared to the Nested Tucker based receivers developed in [13] without performance degradation. Moreover, essential uniqueness of the channel and symbol matrices is ensured up to a scalar factor for each matrix.

The rest of this paper is organized as follows. In Section II, some useful notation and properties are introduced and the basic material on tensor decompositions is given. In Section III, we present the system model and formulate the received signal using the proposed tensor formalism. Section

B. Sokal and A. L. F. de Almeida are with the Wireless Telecom Research Group (GTEL), Department of Teleinformatics Engineering (DETI), Federal University of Ceará (UFC), Fortaleza, Brazil. E-mails: brunosokal@gmail.com, andre@gtel.ufc.br.

M. Haardt is with Ilmenau University of Technology, Communications Research Laboratory, Ilmenau, Germany. E-mail: martin.haardt@tu-ilmenau.de.

This work was supported by FUNCAP and CNPq.

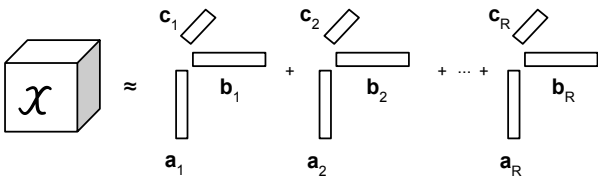


Fig. 1. Illustration of a PARAFAC decomposition as a sum of outer products.

IV presents the proposed Tri-ALS and T-HOSVD receivers. In Section V, simulations are presented and discussed. Finally, Section VI draws the final conclusions and perspectives.

## II. TENSOR DECOMPOSITIONS

### A. Notation and Properties

Scalars are denoted by lower-case letters ( $a, b, \dots$ ), vectors by bold lower-case letters ( $\mathbf{a}, \mathbf{b}, \dots$ ), matrix by bold upper-case letters ( $\mathbf{A}, \mathbf{B}, \dots$ ), tensors are defined by calligraphic upper-case letters ( $\mathcal{A}, \mathcal{B}, \dots$ ). The  $\text{vec}(\cdot)$  operator vectorizes a matrix by stacking its columns, while  $\text{unvec}(\cdot)$  does the inverse operation. The tensorization of a vector  $\mathbf{x} \in \mathbb{C}^{I_1 I_2 I_3 \times 1}$  into a third-order tensor yields  $\mathcal{X}^{I_1 \times I_2 \times I_3}$ .  $\mathbf{A}^T$ ,  $\mathbf{A}^\dagger$ ,  $\mathbf{A}^*$ ,  $\mathbf{A}^H$  stand for transpose, Moore-Penrose pseudo-inverse, conjugate and hermitian of  $\mathbf{A}$ , respectively. The operators  $\otimes$ ,  $\diamond$  and  $\circ$  define the Kronecker, Khatri-Rao and the outer product, respectively. For a fourth order tensor  $\mathcal{X} \in \mathbb{C}^{I_1 \times I_2 \times I_3 \times I_4}$ , we can define two subsets of modes, for example  $S_1 = \{I_1, I_2\}$  and  $S_2 = \{I_3, I_4\}$  and form a matrix  $\mathbf{X}_{I_1 I_2 \times I_3 I_4}$ , whose elements are mapped from  $\mathcal{X}$  according to the little-endian convention [14]. For an  $N$ -th order tensor  $\mathcal{X} \in \mathbb{C}^{I_1 \times \dots \times I_N}$ , its  $n$ -mode matrix unfolding  $\mathbf{X}_{(n)}$  is obtained by taking  $S_1 = \{I_n\}$  and  $S_2 = \{I_1 \dots I_{n-1} I_{n+1} \dots I_N\}$ . The  $n$ -mode product between a tensor  $\mathcal{X} \in \mathbb{C}^{I_1 \times \dots \times I_N}$  and a matrix  $\mathbf{A} \in \mathbb{C}^{J_n \times I_n}$  is defined as  $\mathcal{Y} = \mathcal{X} \times_1 \mathbf{A}$ , where  $\mathcal{Y}^{J_1 \times I_2 \times I_3}$ , so that  $\mathbf{Y}_{(n)} = \mathbf{A} \mathbf{X}_{(n)}$ . Consider two third-order tensors  $\mathcal{X} \in \mathbb{C}^{I_1 \times R \times I_2}$  and  $\mathcal{Y} \in \mathbb{C}^{R \times J_1 \times J_2}$ , where the dimension of the 2-mode of  $\mathcal{X}$  is equal to the dimension of the 1-mode of  $\mathcal{Y}$ . The (2,1)-mode contraction between these two tensors

is symbolized by  $\mathcal{G} = \mathcal{X} \bullet_2^1 \mathcal{Y}$ , i.e.  $g_{i_1 i_2 j_1 j_2} = \sum_{r=1}^R x_{i_1 r i_2} y_{r j_1 j_2}$ ,

where  $\mathcal{G} \in \mathbb{C}^{I_1 \times I_2 \times J_1 \times J_2}$ . A rank-one third-order tensor is defined as the outer product of three vectors and is symbolized by  $\mathcal{X}^{I_1 \times I_2 \times I_3} = \mathbf{a} \circ \mathbf{b} \circ \mathbf{c}$ , with  $\mathbf{a} \in \mathbb{C}^{I_1 \times 1}$ ,  $\mathbf{b} \in \mathbb{C}^{I_2 \times 1}$ ,  $\mathbf{c} \in \mathbb{C}^{I_3 \times 1}$ . Note that  $\text{vec}(\mathbf{a} \circ \mathbf{b} \circ \mathbf{c}) = \mathbf{c} \otimes \mathbf{b} \otimes \mathbf{a}$ . We make use of two useful properties involving the Kronecker product. For matrices  $\mathbf{A}$ ,  $\mathbf{B}$  and  $\mathbf{C}$  of compatible dimensions, we have

$$\text{vec}(\mathbf{ABC}) = (\mathbf{C}^T \otimes \mathbf{A}) \text{vec}(\mathbf{B}). \quad (1)$$

### B. PARAFAC decomposition

The PARAFAC decomposition of  $\mathcal{X}^{I_1 \times I_2 \times I_3}$  is given by

$$\mathcal{X} = \mathcal{I}_{3,R} \times_1 \mathbf{A} \times_2 \mathbf{B} \times_3 \mathbf{C}, \quad (2)$$

where  $\mathcal{I}_{3,R}$  is a diagonal tensor of order 3 and dimension  $R$ ,  $\mathbf{A} \in \mathbb{C}^{I_1 \times R}$ ,  $\mathbf{B} \in \mathbb{C}^{I_2 \times R}$ ,  $\mathbf{C} \in \mathbb{C}^{I_3 \times R}$  are the factor matrices, and  $R$  is the tensor rank. Figure 1 provides an illustration of the PARAFAC decomposition as a sum of outer products involving the columns of the corresponding factor matrices.

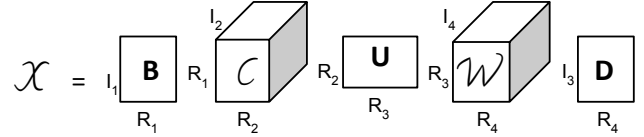


Fig. 2. 3-D illustration of a 4-D Nested Tucker tensor.

The PARAFAC decomposition can be written as a function of its 1-mode, 2-mode and 3-mode unfoldings as follows

$$\mathbf{X}_{(1)} = \mathbf{A}(\mathbf{C} \diamond \mathbf{B})^T \in \mathbb{C}^{I_1 \times I_2 I_3} \quad (3)$$

$$\mathbf{X}_{(2)} = \mathbf{B}(\mathbf{C} \diamond \mathbf{A})^T \in \mathbb{C}^{I_2 \times I_1 I_3} \quad (4)$$

$$\mathbf{X}_{(3)} = \mathbf{C}(\mathbf{B} \diamond \mathbf{A})^T \in \mathbb{C}^{I_3 \times I_1 I_2}. \quad (5)$$

### C. Tucker decomposition

The Tucker decomposition of  $\mathcal{X} \in \mathbb{C}^{I_1 \times I_2 \times I_3}$  is given by

$$\mathcal{X} = \mathcal{G} \times_1 \mathbf{A} \times_2 \mathbf{B} \times_3 \mathbf{C}, \quad (6)$$

where  $\mathcal{G} \in \mathbb{C}^{P \times Q \times R}$  is the core tensor, and  $\mathbf{A} \in \mathbb{C}^{I_1 \times P}$ ,  $\mathbf{B} \in \mathbb{C}^{I_2 \times Q}$  and  $\mathbf{C} \in \mathbb{C}^{I_3 \times R}$ , are the factor matrices. The Tucker-2 decomposition is a special case of (6) with  $\mathbf{C} = \mathbf{I}_R$ , yielding  $\mathcal{X} = \mathcal{G} \times_1 \mathbf{A} \times_2 \mathbf{B}$ . The Tucker-1 decomposition corresponds to having  $\mathbf{B} = \mathbf{I}_Q$  and  $\mathbf{C} = \mathbf{I}_R$ , yielding  $\mathcal{X} = \mathcal{G} \times_1 \mathbf{A}$ .

### D. Nested Tucker decomposition

The Nested Tucker decomposition of a fourth-order tensor  $\mathcal{X} \in \mathbb{C}^{I_1 \times I_2 \times I_3 \times I_4}$  with factor matrices as  $\mathbf{B} \in \mathbb{C}^{I_1 \times R_1}$ ,  $\mathbf{U} \in \mathbb{C}^{R_2 \times R_3}$ ,  $\mathbf{D} \in \mathbb{C}^{I_3 \times R_4}$  and core tensors  $\mathcal{C} \in \mathbb{C}^{R_1 \times R_2 \times I_2}$ ,  $\mathcal{W} \in \mathbb{C}^{R_3 \times R_4 \times I_4}$ ; can be written as [13]

$$\mathcal{X} = \mathcal{T}^{(1)} \bullet_2^1 \mathcal{T}^{(2)} \in \mathbb{C}^{I_1 \times I_2 \times I_3 \times I_4}, \quad (7)$$

where the tensors  $\mathcal{T}^{(1)}$  and  $\mathcal{T}^{(2)}$  are given by:

$$\mathcal{T}^{(1)} = \mathcal{C} \times_1 \mathbf{B} \times_2 \mathbf{U}^T \in \mathbb{C}^{I_1 \times R_3 \times I_2} \quad (8)$$

$$\mathcal{T}^{(2)} = \mathcal{W} \times_2 \mathbf{D} \in \mathbb{C}^{R_3 \times I_3 \times I_4}. \quad (9)$$

Note that  $\mathcal{T}^{(1)}$  and  $\mathcal{T}^{(2)}$  follows a Tucker-2 and Tucker-1 decompositions, respectively. Therefore, the Nested Tucker decomposition can be seen as the contraction between Tucker-1 and Tucker-2 tensors. This decomposition is illustrated in Figure 2.

## III. SYSTEM MODEL

### A. Modeling preliminaries

Consider a one-way two hop MIMO relaying system, where  $M_S$  and  $M_D$  denote the number of antennas at the source and destination, respectively. We assume that the relay has  $M_{R_1}$  receive antennas (operating during the first hop) and  $M_{R_2}$  transmit antennas (operating during the second hop). Figure 3 provides an illustration of the system model. The source-relay channel  $\mathbf{H}^{(SR)} \in \mathbb{C}^{M_S \times M_{R_1}}$  and the relay-destination  $\mathbf{H}^{(RD)} \in \mathbb{C}^{M_D \times M_{R_2}}$  are assumed to undergo flat Rayleigh fading and are constant during the whole transmission period. At both the source and relay, space-time coding is assumed. Let  $\mathbf{S} \in \mathbb{C}^{N \times R}$  denote the symbol matrix containing  $R$  data streams with  $N$  symbols each. At the source, these  $R$  data streams are jointly spread across  $M_S$  antennas and  $P$  time slots by means of a space-time coding tensor

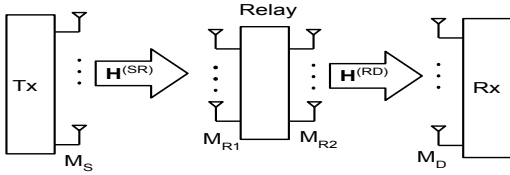


Fig. 3. System model.

$\mathcal{C} \in \mathbb{C}^{R \times M_S \times P}$ . A space-time redundancy is then created since each symbol is repeated  $P$  times and loaded into all  $M_S$  antennas. The signal received at the relay (in absence of noise) can be written as

$$\mathcal{X}^{(SR)} = \mathcal{C}^{(1)} \times_1 \mathbf{S} \times_2 \mathbf{H}^{(SR)\top} \in \mathbb{C}^{N \times M_{R_1} \times P}. \quad (10)$$

In the second hop, the source stays silent while the relay forwards a space-time coded version of the received signal to the destination. Let  $\mathcal{W} \in \mathbb{C}^{M_{R_1} \times M_{R_2} \times J}$  denote the space-time coding tensor used at the relay. The coded signal is given as:

$$\bar{\mathcal{X}}^{(SR)} = \mathcal{X}^{(SR)} \bullet_{\frac{1}{2}} \mathcal{W} \in \mathbb{C}^{N \times P \times M_{R_2} \times J} \quad (11)$$

In a way similar to the first hop, the role of tensor  $\mathcal{W}$  is to jointly spread the received signal across  $M_{R_2}$  transmit antennas and  $J$  time frames, where each time frame comprises  $P$  time slots. At the destination, the noiseless received signal is then given as

$$\mathcal{X}^{(SRD)} = \bar{\mathcal{X}}^{(SR)} \times_3 \mathbf{H}^{(RD)} \quad (12)$$

Define  $\bar{\mathcal{H}}^{(RD)}$  as the space-time coded channel linking the  $M_{R_2}$  relay antennas to the  $M_D$  destination antennas:

$$\bar{\mathcal{H}}^{(RD)} = \mathcal{W} \times_2 \mathbf{H}^{(RD)} \in \mathbb{C}^{M_{R_1} \times M_D \times J} \quad (13)$$

Plugging (11) into (12), and using (13), we get:

$$\begin{aligned} \mathcal{X}^{(SRD)} &= (\mathcal{X}^{(SR)} \bullet_{\frac{1}{2}} \mathcal{W}) \times_3 \mathbf{H}^{(RD)} \\ &= \mathcal{X}^{(SR)} \bullet_{\frac{1}{2}} (\mathcal{W} \times_2 \mathbf{H}^{(RD)}) \\ &= \mathcal{X}^{(SR)} \bullet_{\frac{1}{2}} \bar{\mathcal{H}}^{(RD)} \in \mathbb{C}^{N \times P \times M_D \times J}. \end{aligned} \quad (14)$$

Comparing (14) with (7) we conclude that the signal received at the destination follows a Nested Tucker model, and the following correspondences can be established:

$$(\mathcal{T}^{(1)}, \mathcal{T}^{(2)}) \iff (\mathcal{X}^{(SR)}, \bar{\mathcal{H}}^{(RD)}) \quad (15)$$

$$(\mathbf{B}, \mathbf{U}, \mathbf{D}) \iff (\mathbf{S}, \mathbf{H}^{(SR)}, \mathbf{H}^{(RD)}) \quad (16)$$

$$(I_1, I_2, I_3, I_4) \iff (N, P, M_D, J) \quad (17)$$

$$(R_1, R_2, R_3, R_4) \iff (R, M_S, M_{R_1}, M_{R_2}) \quad (18)$$

Slicing the received signal tensor  $\mathcal{X}^{(SRD)}$  by fixing the second and fourth modes (i.e.  $p$  and  $j$ ) yields the following

$$\mathbf{X}_{\cdot, p, j}^{(SRD)} = \mathbf{S} \mathbf{C}_{\cdot, p} \mathbf{H}^{(SR)} \mathbf{W}_{\cdot, j} \mathbf{H}^{(RD)\top} \in \mathbb{C}^{N \times M_D} \quad (19)$$

Let  $\mathbf{x}_{pj} \doteq \text{vec}(\mathbf{X}_{\cdot, p, j}^{(SRD)})$ . Using Property (1), we have:

$$\begin{aligned} \mathbf{x}_{pj} &= (\mathbf{H}^{(RD)} \otimes \mathbf{S}) \text{vec}(\mathbf{C}_{\cdot, p} \mathbf{H}^{(SR)} \mathbf{W}_{\cdot, j}) \\ &= (\mathbf{H}^{(RD)} \otimes \mathbf{S}) (\mathbf{W}_{\cdot, j}^\top \otimes \mathbf{C}_{\cdot, p}) \text{vec}(\mathbf{H}^{(SR)}) \end{aligned} \quad (20)$$

Applying again the same property in (20) yields

$$\mathbf{x}_{pj} = (\text{vec}(\mathbf{H}^{(SR)})^\top \otimes \mathbf{H}^{(RD)} \otimes \mathbf{S}) \text{vec}(\mathbf{W}_{\cdot, j}^\top \otimes \mathbf{C}_{\cdot, p}) \quad (21)$$

### B. Noisy model and rank-one tensor formulation

Let  $\mathcal{V}^{(SR)} \in \mathbb{C}^{N \times M_{R_1} \times P}$  be the additive noise tensor at the relay. The overall noise at the destination is given by  $\mathcal{V}^{(SRD)} = \mathcal{V}^{(1)} + \mathcal{V}^{(2)}$ , where  $\mathcal{V}^{(1)} = \mathcal{V}^{(SR)} \bullet_{\frac{1}{2}} \bar{\mathcal{H}}^{(RD)} \in \mathbb{C}^{N \times P \times M_D \times J}$  is the filtered noise that is forwarded by the relay, while  $\mathcal{V}^{(2)} \in \mathbb{C}^{N \times P \times M_D \times J}$  is the additive noise term at the destination. Defining  $\mathbf{X} \doteq [\mathbf{x}_{11}, \dots, \mathbf{x}_{P1}, \dots, \mathbf{x}_{PJ}] \in \mathbb{C}^{NM_D \times PJ}$  as a matrix collecting the received signals during  $PJ$  time slots, and including the noise term, we arrive at the following compact representation

$$\mathbf{X} = \mathbf{Y}\mathbf{Z} + \mathbf{V}, \quad (22)$$

where  $\mathbf{Y} \in \mathbb{C}^{NM_D \times RM_{R_2}M_S M_{R_1}}$  and  $\mathbf{Z} \in \mathbb{C}^{RM_{R_2}M_S M_{R_1} \times PJ}$  are ‘‘Kronecker-structured’’ matrices defined as

$$\mathbf{Y} \doteq \text{vec}(\mathbf{H}^{(SR)})^\top \otimes \mathbf{H}^{(RD)} \otimes \mathbf{S} \quad (23)$$

$$\mathbf{Z} \doteq [\text{vec}(\mathbf{W}_{\cdot, 1}^\top \otimes \mathbf{C}_{\cdot, 1}), \dots, \text{vec}(\mathbf{W}_{\cdot, J}^\top \otimes \mathbf{C}_{\cdot, P})], \quad (24)$$

and  $\mathbf{V} \in \mathbb{C}^{NM_D \times PJ}$  is the unfolding matrix of the global noise, which is constructed in the same way as  $\mathbf{X}$ .

It is worth drawing a comment on the meaning of matrices  $\mathbf{Y}$  and  $\mathbf{Z}$ . The first involves the Kronecker product of the unknown factors of our system model (i.e. channel matrices and symbol matrix), which we seek to estimate. The latter represents the equivalent space-time coding matrix, accounting for the combined source-relay coding operations. In other words, (22) provides an input-output relation. Since the coding tensors  $\mathcal{C}$  and  $\mathcal{W}$  are known at the receiver, a direct approach to estimate the useful signal matrix  $\mathbf{Y}$  in the presence of noise from (22) is to use a least squares (LS) criterion, i.e.

$$\hat{\mathbf{Y}} = \underset{\mathbf{Y}}{\text{argmin}} \|\mathbf{X} - \mathbf{Y}\mathbf{Z}\|_F, \quad (25)$$

the solution of which is given by  $\hat{\mathbf{Y}} = \mathbf{X}\mathbf{Z}^\dagger$ . Note that  $\hat{\mathbf{Y}}$  is a linearly transformed version of the received signal obtained by combining (filtering) the columns of the matrix  $\mathbf{X}$  containing the space-time samples of the received signal with a zero forcing filter designed from the effective space-time coding matrix  $\mathbf{Z}$ . Let us have a closer look at the structure of  $\hat{\mathbf{Y}}$ . This matrix can be partitioned as follows

$$\hat{\mathbf{Y}} = \begin{bmatrix} \mathbf{P}_{(1,1)} & \cdots & \mathbf{P}_{(1, M_{R_2} M_S M_{R_1})} \\ \vdots & \vdots & \vdots \\ \mathbf{P}_{(M_D, 1)} & \cdots & \mathbf{P}_{(M_D, M_{R_2} M_S M_{R_1})} \end{bmatrix}, \quad (26)$$

i.e.,  $\hat{\mathbf{Y}}$  can be viewed as a concatenation of  $M_D$  row blocks and  $M_{R_2} M_S M_{R_1}$  column blocks, respectively, where the  $(i, j)$ -th block  $\mathbf{P}_{i,j}$  is of size  $N \times R$ .

Let  $\mathbf{p}_{i,j} \doteq \text{vec}(\mathbf{P}_{i,j}) \in \mathbb{C}^{NR \times 1}$ , and collect all the vectorized blocks in an  $NR \times M_D M_{R_2} M_S M_{R_1}$  matrix

$$\bar{\mathbf{P}} \doteq [\mathbf{p}_{1,1}, \dots, \mathbf{p}_{(M_D, 1)}, \dots, \mathbf{p}_{(M_D, M_{R_2} M_S M_{R_1})}],$$

where the index  $i$  varies faster than the index  $j$  in the construction of this matrix. Finally, by vectorizing  $\bar{\mathbf{P}}$ , we obtain a vector  $\bar{\mathbf{p}} \in \mathbb{C}^{NRM_D M_{R_2} M_S M_{R_1} \times 1}$  that admits the following separable Kronecker structure

$$\bar{\mathbf{p}} = \mathbf{h}^{(SR)} \otimes \mathbf{h}^{(RD)} \otimes \mathbf{s}, \quad (27)$$

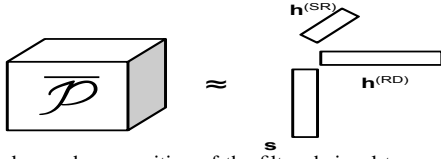


Fig. 4. Rank-one decomposition of the filtered signal tensor.

with  $\mathbf{h}^{(SR)} \in \mathbb{C}^{M_{R_1} M_S \times 1}$ ,  $\mathbf{h}^{(RD)} \in \mathbb{C}^{M_D M_{R_2} \times 1}$ , and  $\mathbf{s} \in \mathbb{C}^{N R \times 1}$  being the vectorized forms of  $\mathbf{S}$ ,  $\mathbf{H}^{(RD)}$  and  $\mathbf{H}^{(SR)}$ , respectively. Since  $\bar{\mathbf{P}}$  corresponds to a Kronecker product of three vectors, its tensorization yields a rank-one third-order tensor  $\bar{\mathcal{P}} \in \mathbb{C}^{N R \times M_D M_{R_2} \times M_{R_1} M_S}$  that can be written as

$$\bar{\mathcal{P}} = \mathbf{s} \circ \mathbf{h}^{(RD)} \circ \mathbf{h}^{(SR)} \in \mathbb{C}^{N R \times M_D M_{R_2} \times M_{R_1} M_S}. \quad (28)$$

#### C. Uniqueness

Solving problem (25) requires  $\mathbf{Z}$  to be full row-rank. Since  $\mathbf{Z} = \mathbf{\Pi}(\mathbf{W}_{(3)} \otimes \mathbf{C}_{(3)})^T \mathbf{\Pi}$ , where  $\mathbf{\Pi}$  is a permutation matrix, we have  $\text{rank}(\mathbf{Z}) = \text{rank}((\mathbf{W}_{(3)} \otimes \mathbf{C}_{(3)})^T) = \text{rank}(\mathbf{W}_{(3)})\text{rank}(\mathbf{C}_{(3)})$ . Hence, a unique recovery of  $\hat{\mathbf{Y}}$  requires  $P \geq R M_S$  and  $J \geq M_{R_1} M_{R_2}$ . Provided that  $\bar{\mathcal{P}}$  is unique,  $\mathbf{s}$ ,  $\mathbf{h}^{(RD)}$ , and  $\mathbf{h}^{(SR)}$  can be estimated up to a scalar factors, i.e.,  $(\hat{\mathbf{S}}, \hat{\mathbf{H}}^{(RD)}, \hat{\mathbf{H}}^{(SR)}) = (\alpha_1 \mathbf{S}, \alpha_2 \mathbf{H}^{(RD)}, \alpha_3 \mathbf{H}^{(SR)})$ , where  $\alpha_1 \alpha_2 \alpha_3 = 1$ . So, in our system, we assume  $\mathbf{S}_{(1,1)} = 1$  and  $\mathbf{H}_{(1,1)}^{(RD)} = 1$  to remove the scalar factor ambiguity.

#### D. Coding structure

Its known that choice of the space-time coding structure affects the receiver performance. In [13], a Vandermonde structure with random generators was chosen for the coding tensors  $\mathcal{C}$  (source) and  $\mathcal{W}$  (relay). We propose the following design procedure. Let  $\mathbf{C}_{(3)} \in \mathbb{C}^{P \times R M_S}$  and  $\mathbf{W}_{(3)} \in \mathbb{C}^{J \times M_{R_1} M_{R_2}}$  be the 3-mode matrix unfoldings of the source and relay coding tensors, respectively. We choose these matrices as discrete Fourier transform (DFT) matrices, such that  $\mathbf{C}_{(3)}^H \mathbf{C}_{(3)} = \mathbf{I}_{R M_S}$  and  $\mathbf{W}_{(3)}^H \mathbf{W}_{(3)} = \mathbf{I}_{M_{R_1} M_{R_2}}$ , i.e.,  $P = R M_S$  and  $J = M_{R_1} M_{R_2}$ . With this choice, it can be shown that the equivalent space-time coding matrix  $\mathbf{Z}$  defined in (24) is unitary, i.e.  $\mathbf{Z}\mathbf{Z}^H = \mathbf{I}_{R M_{R_2} M_S M_{R_1}}$  which means the solution to problem (25) is equivalent to applying a space-time matched filter, i.e.,  $\hat{\mathbf{Y}} = \mathbf{X}\mathbf{Z}^H$ . Such an orthogonal design not only simplifies the receiver processing (by avoiding the computation of the right-inverse of  $\mathbf{Z}$ ), but also yields a better performance compared with the structure proposed in [13].

### IV. SEMI-BLIND RECEIVERS

We present two semi-blind receiver for joint channel and symbol estimation, by capitalizing on the rank-one property of the filtered received signal tensor  $\bar{\mathcal{P}}$ .

#### A. Tri-ALS receiver

The Trilinear (Tri-)ALS algorithm consists of estimating  $\mathbf{s}$ ,  $\mathbf{h}^{(RD)}$ , and  $\mathbf{h}^{(SR)}$  in an alternate way by solving the following three cost functions:

$$\hat{\mathbf{s}} = \underset{\mathbf{s}}{\text{argmin}} \quad \|\bar{\mathbf{P}}_{(1)} - \mathbf{s}(\hat{\mathbf{h}}^{(SR)} \diamond \hat{\mathbf{h}}^{(RD)})^T\| \quad (29)$$

$$\hat{\mathbf{h}}^{(RD)} = \underset{\mathbf{h}^{(RD)}}{\text{argmin}} \quad \|\bar{\mathbf{P}}_{(2)} - \mathbf{h}^{(RD)}(\hat{\mathbf{h}}^{(SR)} \diamond \hat{\mathbf{s}})^T\| \quad (30)$$

$$\hat{\mathbf{h}}^{(SR)} = \underset{\mathbf{h}^{(SR)}}{\text{argmin}} \quad \|\bar{\mathbf{P}}_{(3)} - \mathbf{h}^{(SR)}(\hat{\mathbf{h}}^{(RD)} \diamond \hat{\mathbf{s}})^T\|, \quad (31)$$

#### Algorithm 1 Tri-ALS

- 1: Initialize randomly  $\hat{\mathbf{h}}_0^{(RD)}$  and  $\hat{\mathbf{h}}_0^{(SR)}$ ;  $it = 0$ ;
- 2:  $it = it + 1$ ;
- 3: Calculate an estimate of  $\hat{\mathbf{s}}$   
 $\hat{\mathbf{s}}_{it} = \bar{\mathbf{P}}_{(1)}(\hat{\mathbf{h}}_{it-1}^{(SR)} \diamond \hat{\mathbf{h}}_{it-1}^{(RD)})^* / (\|\hat{\mathbf{h}}_{it-1}^{(SR)}\|_2 \|\hat{\mathbf{h}}_{it-1}^{(RD)}\|_2)$
- 4: Calculate an estimate of  $\hat{\mathbf{h}}^{(RD)}$   
 $\hat{\mathbf{h}}_{it}^{(RD)} = \bar{\mathbf{P}}_{(2)}(\hat{\mathbf{h}}_{it-1}^{(SR)} \diamond \hat{\mathbf{s}}_{it-1})^* / (\|\hat{\mathbf{h}}_{it-1}^{(SR)}\|_2 \|\hat{\mathbf{s}}_{it-1}\|_2)$
- 5: Calculate an estimate of  $\hat{\mathbf{h}}^{(SR)}$   
 $\hat{\mathbf{h}}_{it}^{(SR)} = \bar{\mathbf{P}}_{(3)}(\hat{\mathbf{h}}_{it-1}^{(RD)} \diamond \hat{\mathbf{s}}_{it-1})^* / (\|\hat{\mathbf{h}}_{it-1}^{(RD)}\|_2 \|\hat{\mathbf{s}}_{it-1}\|_2)$
- 6: Return to step 2 and repeat until convergence;
- 7: Remove the scaling ambiguities;
- 8: Apply the “unvec” operator to recover  $\hat{\mathbf{S}}, \hat{\mathbf{H}}^{(RD)}, \hat{\mathbf{H}}^{(SR)}$ .

#### Algorithm 2 T-HOSVD

- 1: For  $n = 1, 2, 3$ :  
 Compute the SVD of the matrix unfolding  $\bar{\mathbf{P}}_{(n)}$ ;  
 $\hat{\mathbf{Y}}^{(n)} = \mathbf{U}_{(n)} \mathbf{\Sigma}_{(n)} \mathbf{V}_{(n)}^H$
- 2: Select the dominant left singular vector from  $\mathbf{U}_{(n)}$ :  
 $\hat{\mathbf{s}} = \alpha_1 \mathbf{U}_{(1)}(:, 1)$ ;  
 $\hat{\mathbf{h}}^{(RD)} = \alpha_2 \mathbf{U}_{(2)}(:, 1)$ ;  
 $\hat{\mathbf{h}}^{(SR)} = \mathbf{U}_{(3)}(:, 1) \frac{\mathbf{\Sigma}_{(3)} \mathbf{V}_{(3)}^*}{\mathbf{S}_{(1,1)} \mathbf{H}_{(1,1)}^{(RD)}}$
- 3: Apply the “unvec” operator to recover  $\hat{\mathbf{S}}, \hat{\mathbf{H}}^{(RD)}, \hat{\mathbf{H}}^{(SR)}$ .

where  $\bar{\mathbf{P}}_{(n=1,2,3)}$ , are the  $n$ -mode unfoldings of the tensor  $\bar{\mathcal{P}}$ , constructed according to equations (3) to (5) with the following relationship:  $(\mathbf{A}, \mathbf{B}, \mathbf{C}) \iff (\mathbf{s}, \mathbf{h}^{(SR)}, \mathbf{h}^{(RD)})$ . The Tri-ALS algorithm is summarized in Algorithm 1.

#### B. T-HOSVD receiver

The Truncated (T)-HOSVD algorithm is a closed-form solution based on subspace estimation. It consists of taking the HOSVD on the filtered received signal tensor  $\bar{\mathcal{P}}$ , which corresponds to calculating the SVD of its matrix unfoldings. Since  $\bar{\mathcal{P}}$  is a rank-one tensor, its three matrix unfoldings can be approximated as rank-one matrices. Therefore,  $\mathbf{s}$ ,  $\mathbf{h}^{(RD)}$ , and  $\mathbf{h}^{(SR)}$  are obtained from the dominant left singular vectors of the unfoldings  $\bar{\mathbf{P}}_{(1)} \in \mathbb{C}^{N R \times M_D M_{R_2} M_S M_{R_1}}$ ,  $\bar{\mathbf{P}}_{(2)} \in \mathbb{C}^{M_D M_{R_2} \times N R M_S M_{R_1}}$ , and  $\bar{\mathbf{P}}_{(3)} \in \mathbb{C}^{M_S M_{R_1} \times N R M_D M_{R_2}}$ . The T-HOSVD algorithm is described in Algorithm 2.

### V. SIMULATION RESULTS

In this section, we evaluate the performance of the proposed receivers in terms of symbol error rate (SER), normalized mean square error (NMSE) for channel estimation, computational complexity, and convergence, comparing with the receivers proposed in [13]. We consider 4-QAM modulation. The results are averaged over  $10^4$  Monte Carlo runs, each run corresponding to an independent realization of the channels, symbols, and noise. The channel matrices are assumed to have i.i.d. complex Gaussian entries with zero-mean and unitary variance.

Figure 5 depicts the performance of the Tri-ALS and T-HOSVD receiver in comparison with the two receivers proposed in [13] (namely, ALS Nested Tucker and 2LSKP receivers), using the proposed DFT structure for the source and relay coding tensors. It can be noticed the two proposed

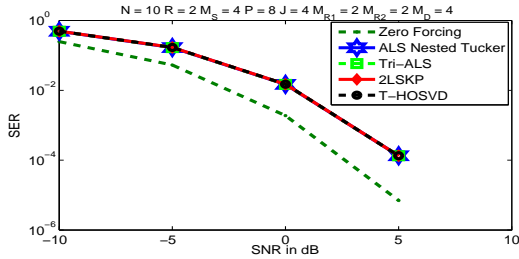


Fig. 5. SER vs. SNR performance.

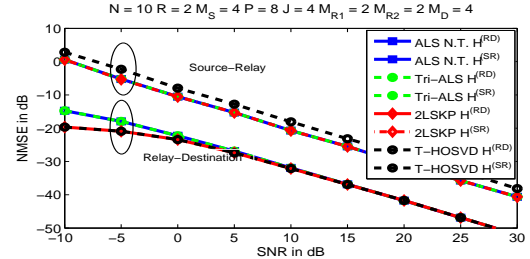


Fig. 6. NMSE of channel estimation.

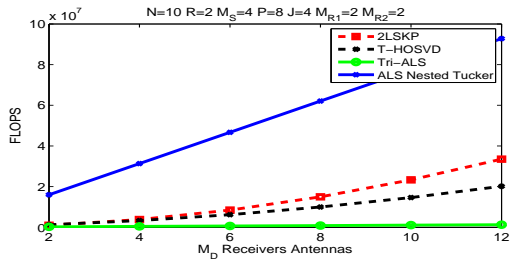
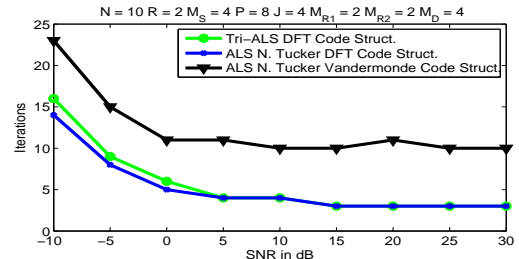

 Fig. 7. Number of FLOPS vs.  $M_D$ .


Fig. 8. Number of iterations for ALS convergence.

receivers reach the same performance as those of [13], while being less complex, as will be shown in the sequel. Figure 6 shows the NMSE performance of the estimated channels. As for the SER performance, the Tri-ALS and T-HOSVD receivers provide the same performance as the Nested Tucker based receivers [13]. We can note that in all cases, the NMSE curves decrease linearly as a function of the SNR. Now, we evaluate the computational complexity of the proposed receivers by measuring the number of floating point operations (FLOPS) required by the different receivers to accomplish joint channel and symbol estimation. To this end, the *lightspeed MATLAB* toolbox [15] was used to count the number of FLOPS. Figure 7 corroborates the benefits of the proposed rank-one tensor based receivers in terms of computational complexity, when compared to the competing receivers. We can note that the Tri-ALS receiver becomes much less complex than its competing Nested Tucker based ALS solution. When it comes to the closed-form receivers, these results show that the T-HOSVD receiver is more attractive than the 2LSKP receiver as the number  $M_D$  of antennas grows. Another advantage of T-HOSVD over 2LSKP is related with parallel implementation. Since the T-HOSVD consists of three independent SVDs, the estimation of the source-relay, relay-destination and symbol matrices can be carried out in parallel. This is not the case of 2LSKP, which consists of two consecutive SVDs steps, where the result of the second step depends on the output of the first. Figure 8 shows the impact of the proposed DFT-based design for the source and relay coding tensors on the convergence of ALS-based receivers. To this end, we compare the proposed Tri-ALS receiver with the Nested Tucker based ALS receiver. For the latter, we consider the Vandermonde structure with random generators, as proposed in [13], and the proposed DFT coding structure. Note that the proposed one yields a reduction on the number of iterations to convergence. For high SNR, the number of iterations reduces approximately from 10 to 3.

## VI. CONCLUSIONS

We have proposed a new tensor modeling approach to the problem of joint channel and symbol estimation in a two-hop MIMO relaying system. Our approach capitalizes on a rank-one tensor modeling of the received signal after space-time combining and yields simple receiver algorithms, which are less complex than the competing solutions proposed in the literature. Perspectives for future work include the generalization to the multi-relay/multihop scenario.

## REFERENCES

- [1] K. J. R. Liu et al., *Cooperative Communications and Networking*. New York, NY, USA: Cambridge University Press, 2009.
- [2] L. Cao, J. Zhang, and N. Kanno, "Multi-user cooperative communications with relay-coding for uplink imt-advanced 4G systems," in *Proc. IEEE GLOBECOM*, 2009, pp. 1–6.
- [3] M. Dohler and Y. Li, *Cooperative communications: hardware, channel and PHY*. John Wiley & Sons, 2010.
- [4] Y. Rong, X. Tang, and Y. Hua, "A unified framework for optimizing linear nonregenerative multicarrier MIMO relay communication systems," *IEEE Trans. on Signal Process.*, vol. 57, pp. 4837–4851, 2009.
- [5] T. Kong and Y. Hua, "Optimal channel estimation and training design for MIMO relays," *Proc. ASILOMAR-SSC, USA*, 2010, pp. 663–667.
- [6] N. D. Sidiropoulos, G. B. Giannakis, and R. Bro, "Blind parafac receivers for DS-CDMA systems," *IEEE Trans. Signal Process.*, vol. 48, no. 3, pp. 810–823, 2000.
- [7] A. L. de Almeida, G. Favier, and J. C. M. Mota, "A constrained factor decomposition with application to mimo antenna systems," *IEEE Trans. Signal Process.*, vol. 56, no. 6, pp. 2429–2442, 2008.
- [8] A. L. de Almeida and G. Favier, "Double khatri-rao space-time-frequency coding using semi-blind PARAFAC based receiver," *IEEE Signal Proc. Letters*, vol. 20, no. 5, pp. 471–474, 2013.
- [9] G. Favier, M. N. da Costa, A. L. de Almeida, and J. M. T. Romano, "Tensor space-time (TST) coding for {MIMO} wireless communication systems," *Signal Processing*, vol. 92, no. 4, pp. 1079–1092, 2012.
- [10] F. Roemer and M. Haardt, "Tensor-based channel estimation and iterative refinements for two-way relaying with multiple antennas and spatial reuse," *IEEE Trans. Signal Process.*, vol. 58, no. 11, pp. 5720–5735, 2010.
- [11] I. V. Cavalcante, A. L. de Almeida, and M. Haardt, "Tensor-based approach to channel estimation in amplify-and-forward mimo relaying systems," *Proc. IEEE Proc. IEEE SAM*, 2014, pp. 445–448.
- [12] L. R. Ximenes, G. Favier, and A. L. de Almeida, "Semi-blind receivers for non-regenerative cooperative MIMO communications based on nested parafac modeling," *IEEE Trans. Signal Process.*, vol. 63, no. 18, pp. 4985–4998, 2015.
- [13] G. Favier, C. A. R. Fernandes, and A. L. de Almeida, "Nested Tucker tensor decomposition with application to MIMO relay systems using tensor space-time coding (TSTC)," *Signal Processing*, vol. 128, pp. 318–331, 2016.
- [14] A. Cichocki, "Tensor networks for big data analytics and large-scale optimization problems," *arXiv preprint 1407.3124*, 2014.
- [15] T. Minka, "The lightspeed MATLAB toolbox: efficient operations for MATLAB programming," *Microsoft Corp.*, vol. 2.2, 2007.